# Recruitment and Endo-Lysosomal Activation of TLR9 in Dendritic Cells Infected with *Trypanosoma cruzi*[1]

**Daniella C. Bartholomeu,[2]* Catherine Ropert,[2†] Mariane B. Melo,[‡] Peggy Parroche,[‡] Caroline F. Junqueira,* Santuza M. R. Teixeira,* Cherilyn Sirois,[‡] Pia Kasperkovitz,[‡] Cathrine F. Knetter,[‡] Egil Lien,[‡] Eicke Latz,[‡] Douglas T. Golenbock,[†] and Ricardo T. Gazzinelli[3]*[†‡]**

**TLR9 is critical in parasite recognition and host resistance to experimental infection with *Trypanosoma cruzi*. However, no information is available regarding nucleotide sequences and cellular events involved on *T. cruzi* recognition by TLR9. In silico wide analysis associated with in vitro screening of synthetic oligonucleotides demonstrates that the retrotransposon VIPER elements and *mucin-like glycoprotein* (TcMUC) genes in the *T. cruzi* genome are highly enriched for CpG motifs that are immunostimulatory for mouse and human TLR9, respectively. Importantly, infection with *T. cruzi* triggers high levels of luciferase activity under NF-κB-dependent transcription in HEK cells cotransfected with human TLR9, but not in control (cotransfected with human MD2/TLR4) HEK cells. Further, we observed translocation of TLR9 to the lysosomes during invasion/uptake of *T. cruzi* parasites by dendritic cells. Consistently, potent proinflammatory activity was observed when highly unmethylated *T. cruzi* genomic DNA was delivered to the endo-lysosomal compartment of host cells expressing TLR9. Thus, together our results indicate that the unmethylated CpG motifs found in the *T. cruzi* genome are likely to be main parasite targets and probably become available to TLR9 when parasites are destroyed in the lysosome-fused vacuoles during parasite invasion/uptake by phagocytes. *The Journal of Immunology,* 2008, 181: 1333–1344.**

Toll-like receptor 9 was identified as an innate immune receptor responsible for recognition of immunostimulatory oligodeoxynucleotides (ODNs)[4] containing unmethylated CpG motifs derived from bacterial DNA (1–3). Identification of similar ODN sequences in viral genomes (3–5) and cellular localization of TLR9 in the endosomal compartment (6) have also indicated the relevance of this innate immune receptor during viral infection. Importantly, in vitro and in vivo experiments demonstrate the contribution of parasite genomic DNA as well as TLR9 to initiate IL-12 and IFN-γ production and host resistance to infection with protozoan parasites (7–10).

*Trypanosoma cruzi*, the causative agent of Chagas disease, is an intracellular parasite. Immunological control of *T. cruzi* during early stages of infection in the vertebrate host is dependent on both innate and acquired cell-mediated immune responses (11). A role for TLR signaling in resistance to *T. cruzi* infection is supported by experiments showing that mice deficient in the myeloid differentiation primary response gene MyD88, an adaptor molecule required for signaling events by most TLRs as well as by IL-1R and IL-18R, show greatly enhanced susceptibility to infection (12). Importantly, mice lacking both TLR2 and TLR9 show impaired IL-12 and IFN-γ synthesis and are also highly susceptible to *T. cruzi* infection (8).

GPI anchors have been previously defined as a major class of *T. cruzi* glycolipids that are recognized by TLRs. The highly purified GPI anchors derived from the mucin-like glycoproteins of trypomastigotes contain unsaturated fatty acid chains as well as a long carbohydrate branch and are potent agonists of TLR2 (13). In addition, a particular subset of free GPI anchors containing ceramide (glycoinositolphospholipid ceramide) has been shown to stimulate macrophage proinflammatory cytokine production via TLR4 (14). Importantly, genomic DNA from both *T. cruzi* and *Trypanosoma brucei* stimulate cytokine responses from macrophages and dendritic cells (DCs) (15), suggesting that DNA from trypanosomatids contain sufficient unmethylated CpG motifs to induce activation of host cells via TLR9 (7, 8, 16). However, immunostimulatory DNA sequences in the genomes of protozoan parasites have not been identified, and the cellular compartment in which *Trypanosoma* DNA encounters TLR9 remains unsolved.

We identified immunostimulatory ODNs containing CpG motifs in the *T. cruzi* genome. Interestingly, the retrotransposon VIPER element (mouse-motif) and the *mucin-like glycoprotein TcMUC* (human-motif), which are associated with regions of the genome

*Department of Parasitology and Department of Biochemistry and Immunology, Institute of Biological Sciences, Federal University of Minas Gerais, Belo Horizonte, Minas Gerais, Brazil; †René Rachou Institute, Oswaldo Cruz Foundation, Belo Horizonte, Minas Gerais, Brazil; and ‡Division of Infectious Disease and Immunology, Department of Medicine, University of Massachusetts Medical School, Worcester, MA 01655

Received for publication March 28, 2008. Accepted for publication May 5, 2008.

The costs of publication of this article were defrayed in part by the payment of page charges. This article must therefore be hereby marked *advertisement* in accordance with 18 U.S.C. Section 1734 solely to indicate this fact.

[1] This work was supported by Atlantic Philanthropies and the Ludwig Institute for Cancer Research, the Millennium Institute for Technology and Vaccine Development/Conselho Nacional de Desenvolvimento Cientifico e Technologico (CNPq), Fundacao de Amparo a Pesquisa do Estado de Minas Gerais (FAPEMIG), and the National Institutes of Health (Grant AI071319-01). D.C.B. is supported by the World Health Organization/Special Program for Training in Tropical Diseases and FAPEMIG. R.T.G., D.C.B., S.M.R.T., and C.R. are research fellows from CNPq and FAPEMIG, respectively.

[2] D.C.B. and C.R. contributed equally to this work.

[3] Address correspondence and reprint requests to Dr. Ricardo T. Gazzinelli, Laboratory of Immunopathology, René Rachou Institute, Oswaldo Cruz Foundation (FIOCRUZ), Av. Augusto de Lima 1715, 30190-002 Belo Horizonte, Minas Gerais, Brazil. E-mail address: ritoga@cpqrr.fiocruz.br

[4] Abbreviations used in this paper: ODN, oligodeoxynucleotide; BMDC, bone marrow-derived dendritic cell; DC, dendritic cell; DOTAP, 1,2-dioleoyloxy-3-(trimethylammonium)propane; RFP, red fluorescent protein; WT, wild type; YFP, yellow fluorescent protein.

Table I. *Sequence, expected number of copies, and annotation of mouse and human stimulatory B-class-like CpG motifs present in the* T. cruzi *genome*[a]

| Name | Sequence (5′ to 3′) | Expected No. of Copies | Annotation Sense (S)/Antisense (AS) | Stimulatory Index TLR9 | |
|---|---|---|---|---|---|
| | | | | Mouse | Human |
| Mouse CpG-B-class-like motifs | | | | | |
| B-class_616 | TCGACGTTTGGATCGAT | 44 | 57 VIPER (S) | 146 | 6 |
| B-class_344 | TCGACGTTTGGATCGGT | 24.6 | 31 VIPER (S), 1 L1Tc | 125 | 5 |
| B-class_772 | TCGACGTATGGATCGAT | 55.1 | 61 VIPER (S) | 76 | 5 |
| B-class_597 | TCGACGTATGGATCGGT | 42.6 | 21 VIPER (S), 1 NULL | 75 | 5 |
| Mouse-human hybrid CpG-B class-like motif | | | | | |
| B-class_297 | TCCTCGTTTTGACGTG | 21.2 | 13 HP (AS); 2 TS $\psi$, putative (AS); 1 HP $\psi$ (AS); 1 MASP $\psi$ (AS) | 133 | 3 |

[a] HP, Hypothetical protein; $\psi$, pseudogene; TS, *trans*-sialidase; MASP, mucin-associated surface protein; L1Tc, *T. cruzi* non-LTR retrotransposon; NULL, noncoding region. Numbers preceding gene code/name indicate the number of copies of this specific gene that contains a particular CpG motif. Stimulatory Index" indicates the percentage of responses relative to the responses to the positive control stimulatory oligonucleotide for mouse (CpG 7909) or human (CpG 2007). The B-class stimulatory oligonucleotide activities were determined in a NF-κB dependent luciferase activity in HEK cells stably transfected with either human or mouse TLR9. B-class-like ODNs were synthesized in a phosphorothioate backbone.

that are specific for *T. cruzi* (i.e., not syntenic with *T. brucei* and *Leishmania major* genomes), were enriched for these sequences. Further, we evidenced TLR9 signaling in host cells infected with *T. cruzi*. Colocalization of TLR9 and *T. cruzi* parasites occurs within vacuoles containing lysosomal-associated membrane protein 1 (LAMP-1), an endo-lysosomal marker. Preactivation of DCs with immunostimulatory ODNs promoted the encounter of TLR9 and parasites in the lysosomes that are recruited by the parasite during the initial steps of the invasion process. Importantly, we show that TLR9 stimulatory activity is much enhanced when *T. cruzi* genomic DNA is delivered into the endo-lysosomal compartments of host cells. Thus, our study defines main parasite targets and the cellular compartment likely to be involved upon *T. cruzi* recognition by TLR9 and the induction of IL-12 as well as IFN-γ synthesis and the consequent host resistance to infection with this protozoan parasite.

## Materials and Methods

All animal and human studies were approved by the Institutional Review Boards of the René Rachou Institute, Oswaldo Cruz Foundation, Belo Horizonte, Minas Gerais, Brazil, and University of Massachusetts Medical School, Worcester, MA.

### *TLR agonists and other reagents used in cellular assays*

LPS from *Escherichia coli* strain 0111:B4 was purchased from Sigma-Aldrich and re-extracted by phenol (17). PMA and ionomycin were also purchased from Sigma-Aldrich. TNF-α was purchased from BD Biosciences. R848, a synthetic small molecule agonist for TLR7 was provided by 3M Pharmaceuticals. The ODNs identified in the *T. cruzi* genome and presented in Tables I and II, the 7909 CpG or the GpG inactive ODNs, were synthesized by Alpha DNA as phosphorothioate ODNs. ODNs 2007 (B-class CpG), 2137 (B-class GpC), 2336 (A-class CpG), 2243 (A-class GpC), and 2395 (C-class CpG) were purchased from Coley Pharmaceutics. *N*-[1-(2,3-Dioleoyloxy)propyl]-*N*,*N*,*N*-trimethylammonium methylsulfate (DOTAP), a liposomal transfection reagent (Roche Diagnostics), was used according to manufacturer's instructions (9) for the stimulation of cells with ODNs or DNA.

### *Parasites*

The CL-Brener strain of *T. cruzi* (18) was continuously passed as blood trypomastigote forms in Swiss outbred mice or maintained as epimastigotes in logarithmic growth phase at 28°C in liver infusion tryptose medium supplemented with 10% FBS (19). The transgenic CL-Brener strain expressing red fluorescence protein (RFP) was generated using the plasmid pROCKRFPNeo, which promotes the integration of a cassette for foreign gene expression and the neomycin resistance gene NeoR into the β-tubulin locus (20–22). Transfected epimastigotes were maintained in liver infusion tryptose medium under drug selection using 200 μg of G418. The metacyclic stages expressing RFP were used to infect Vero fibroblast cells to generate tissue culture trypomastigotes expressing RFP (23). Cell lines and parasites were routinely tested for *Mycoplasma* with a PCR *Mycoplasma* test kit (MD Biosciences).

### *Genomic DNA parasite preparations*

Genomic DNA was purified from epimastigotes using the GFXTM genomic DNA purification kit (GE Healthcare). Purified DNA was digested with DNase I (Invitrogen) (9) or CpG M.SssI methylase (New England Biolabs) (15) and stored at −20°C until use. Complete digestion of DNA and DNA methylation, as determined by resistance to cleavage by *Hpa*II (New England Biolabs), was confirmed by agarose gel electrophoresis. Concentrations of DNA were determined and tested for the presence of endotoxin by *Limulus* amebocyte lysate assay (BioWhittaker).

### *Cell populations*

Mouse bone marrow-derived DCs (BMDCs) from C57BL/6, TLR9$^{-/-}$, TLR4$^{-/-}$ or MyD88$^{-/-}$ mice (8) were cultured in complete medium supplemented with 10% of culture supernatant from the J558L cell line, which contains GM-CSF (24). After 6 days of culture, $1 \times 10^5$ cells were seeded in each well in 96-well plates for in vitro experiments. In some experiments the murine BMDCs were transduced. For retroviral transduction, recombinant virus was produced by cotransfecting 293T cells with a peak12mmp plasmid encoding yellow fluorescent protein (YFP)-tagged TLR9 (5.5 μg), plasmids carrying the retroviral *gag-pol* genes (5.5 μg), and the envelope protein VSV-G (1 μg). BMDCs were transduced on day 2 of culture and analyzed by confocal microscopy on day 8. Mice injected with 1.5 ml of 3% thioglycolate were as used as source of inflammatory macrophages (23). Peripheral blood samples drawn from healthy donors were submitted to Ficoll-Paque Plus (GE Healthcare) fractionation to obtain PBMCs. HEK-TLR4-cyan fluorescent protein/MD2, HEK-TLR9-YFP (6), HEK cells stably transfected with both human TLR9 or TLR7 and luciferase under the control of a pELAM promoter (25), and HEK cells stably transfected with mouse TLR9-YFP (C.F. Knetter and E. Lien, unpublished observations) were used to test the activity of ODN CpG motifs.

### *Experimental infections with* T. cruzi

The TLR9$^{-/-}$ mice were obtained from Dr. S. Akira (Osaka University, Osaka, Japan) and backcrossed into C57BL/6 mice for at least eight generations. Eight-week-old male mice were i.p. infected with 1,000 blood trypomastigotes of *T. cruzi*, parasitemia was evaluated by counting parasites in 5 μl of blood from the tail vein, and mortality was assessed daily.

### *Genome mining for islands containing CpG stimulatory motifs*

Genome mining was performed using the individual reads generated in the *T. cruzi* genome project (18) to keep the representation of repetitive sequences that were not incorporated in the assembled data. A total of 1,192,680 reads totaling 768,436,632 nucleotides (14× genome coverage) were searched for the three known classes of immunostimulatory CpG DNA motifs (26) using the fuzznuc algorithm (EMBOSS package). The fuzznuc reverse option was turned on so that both DNA

Table II. *Sequence, expected number of copies, and annotation of human stimulatory A-, B- and C-class-like stimulatory CpG motifs present in the* T. cruzi *genome*[a]

| Name | Sequence (5′ to 3′) | Expected No. of Copies | Annotation Sense (S)/Antisense (AS) | Stimulatory Index TLR9 | |
|---|---|---|---|---|---|
| | | | | Mouse | Human |
| Human A-class-like CpG motifs | | | | | |
| A-class_56 | GGGGCCCGTGCCGGCAACGGGG | 4.0 | 4 HP (S) | 7 | 5 |
| A-class_32 | GGGGGAGGGCGGCCGGCGCGCCGGGGG | 2.3 | NULL | 5 | 4 |
| A-class_25 | GGGGGCGCCCGCAGCGGGG | 1.8 | 2 Mucin-like glycoprotein (S); 1 HP (S) | 3 | 5 |
| A-class_24 | GGGGCTCCGCGGTGGCCGCGGGG | 1.7 | NULL | 5 | 4 |
| A-class_22 | GGGGGACGATAACGTTATGGGGG | 1.6 | NULL | 10 | 4 |
| A-class_19 | GGGGCCGTACGAACGGCGGGG | 1.4 | 2 HP-C (AS) | 6 | 4 |
| A-class_16 | GGGGGCGTCCCCGTGCGGGG | 1.1 | 1 HP-C (AS); 1 NULL | 5 | 4 |
| A-class_15A | GGGGGCGGGTCGAGCGCTCGGGG | 1.1 | 1 HP-C (S) | 7 | 5 |
| A-class_15B | GGGGACGGCCGTCGGGG | 1.1 | 2 Serine/threonine protein kinase (AS) | 4 | 2 |
| A-class_14 | GGGGCCTCGCGGTACCCGCTGCGGGG | 1.0 | 2 HP-C (S) | 5 | 2 |
| Human B-class-like CpG motifs | | | | | |
| B-class_377 | TCGTCGTTGTCGTC | 26.9 | 15 HP-C (AS); 5 TcMUC II, putative (AS); 3 TcSMUGS, putative (AS); 1 TS (AS); 1 HP-C (S); 3 NULL | 45 | 65 |
| B-class_181 | TTGTCGTTGTCGTT | 12.9 | 5 TcMUC II, putative (AS); 2 HP-C (AS); 1 PI3K $\psi$, putative (AS); 1 HP-C $\psi$ (AS); 1 (2) dual specificity protein phosphatase, putative (AS); 1 HP-C (S); 14 NULL | 11 | 16 |
| B-class_145 | TTGTCGTCGTCGTT | 10.4 | 2 TcMUC $\psi$, putative (AS); 2 HP-C (AS); 1 HP-C $\psi$ (AS); 10 NULL | 6 | 16 |
| B-class_138A | TTGTCGTAGTCGTCGTT | 9.9 | 9 TcMUC II $\psi$, putative (AS); 7 TcMUC II, putative (AS); 1 TcMUC $\psi$, putative (AS) | 8 | 35 |
| B-class_138B | TCGTCGTCGTCGTT | 9.9 | 4 HP-C (AS); 2 HP (AS); 2 CDC45, putative (AS); 1 myosin heavy chain MYA2-related, putative (AS); 1 TcMUC II, putative (AS); 3 HP-C (S); 1 paraflagellar rod protein, putative (S); 2 NULL | 9 | 61 |
| B-class_130 | TCGTCGTTGTCGTT | 9.3 | 10 TcMUC II, putative (AS); 3 HP-C (AS); 1 TcMUC II $\psi$, putative (AS); 4 NULL | 74 | 86 |
| B-class_128 | TCGTCGTTGTAGTCGTA | 9.1 | 1 TcMUC I, putative (AS) | 100 | 77 |
| B-class_126 | TCGTCGTGGTCGTT | 9.0 | 15 TcMUC II, putative (AS); 1 TcMUC I, putative (AS); 1 TcMUC II $\psi$, putative (AS) | 16 | 49 |
| B-class_114 | TCGTCGTAGTCGTT | 8.1 | 3 TcMUC II $\psi$, putative (AS); 1 HP (AS) | 19 | 47 |
| B-class_110 | TCGTCGTTGTCGTG | 7.9 | 2 TcMUC I, putative (AS); 2 TcMUC II, putative (AS); 1 NULL | 72 | 50 |
| Human C-class-like CpG motifs | | | | | |
| C-class_318 | TCGTCGTATTTGGCGCC | 22.7 | 12 TcMUC I, putative (AS); 1 TcMUC II, putative (AS); 1 TcMUC II $\psi$, putative (AS) | 21 | 28 |
| C-class_197 | GCGTCGTTGCCGCGGC | 14.1 | 1 HP (AS); 21 NULL | 9 | 6 |
| C-class_180 | TCGTCGTTGGAGGCGCC | 12.9 | 1 MASP, putative (S); 1 MASP $\psi$, putative (S); 9 NULL | 47 | 19 |
| C-class_151 | TCGTCGTGGCCGGC | 10.8 | 2 Glycosomal phosphoenolpyruvate carboxykinase, putative (AS); 1 ABC transporter, putative (AS); 7 NULL | 9 | 12 |
| C-class_144 | GCGTCGTTGCCGCGGC | 10.3 | HP (AS); 21 NULL | 11 | 7 |
| C-class_122 | TCGTCGTTGGCGCC | 8.7 | 1 (12) TcMUC I, putative (AS); 3 TcMUC II, putative (AS); 1 (3) HP (AS); 1 HP-C (S); 1 (2) TcMUC I, putative (AS); 1 TcMUC I, putative (AS) | 20 | 23 |
| C-class_76 | TCGTCGTTTTGGGGGCCC | 5.4 | 2 HP-C (S); 4 HP-C $\psi$ (S) | 11 | 18 |
| C-class_70 | TCGTCGTCGCCGGC | 5.0 | 3 DGF-1 $\psi$ (S); 3 DGF-1, putative (S) | 9 | 6 |
| C-class_63 | GCGTCGTTTTGCCGGC | 4.5 | 2 ABC transporter, putative (AS) | 9 | 10 |

[a] HP, Hypothetical protein; HP-C = hypothetical protein, conserved; $\psi$, pseudogene; TcMUC, mucin-like glycoprotein; HSP70, heat shock 70-kDa protein; TS, *trans*-sialidase; MASP, mucin-associated surface protein; CDC, cell division cycle protein; NULL, noncoding region. Numbers preceding the gene code/name indicate the number of copies of this specific gene that contains a particular CpG motif. Numbers within parentheses indicate the number of motifs in a single gene. "Stimulatory Index" indicates the percentage of response relative to the response to positive control stimulatory oligonucleotides for mouse (CpG 7909) and human (CpG 2007). The A-, B-, and C-class-like stimulatory oligonucleotide activities were determined in a NF-$\kappa$B-dependent luciferase activity in HEK cells stably transfected with either human or mouse TLR9. A-class like ODNs were synthesized as poly(G) motifs with phosphorothioate linkages at the 5′ and 3′ ends and phosphotriester palindromic CpG-containing sequences in the ODN center. B- and C-class-like ODNs were synthesized entirely in a phosphorothioate backbone.

strands were searched. In the case of the A- and C-classes, the palindrome algorithm (EMBOSS package) was also included in the pipeline. The identified CpG motifs were then mapped on the annotated contigs.

To identify CpG B-class like motifs slightly distinct from those previously described in bacteria (2), we used the following criteria: 1) the presence of two CpG motifs, each one having the general formula purine-purine or thymine − CpG − pyrimidine − pyrimidine; 2) the two motifs should be spaced with two or three pyrimidine residues; 3) TpC dinucleotide on the 5′ end; and 4) pyrimidine rich on the 3′ side. Three mismatches were allowed as long as they did involve neither one of the

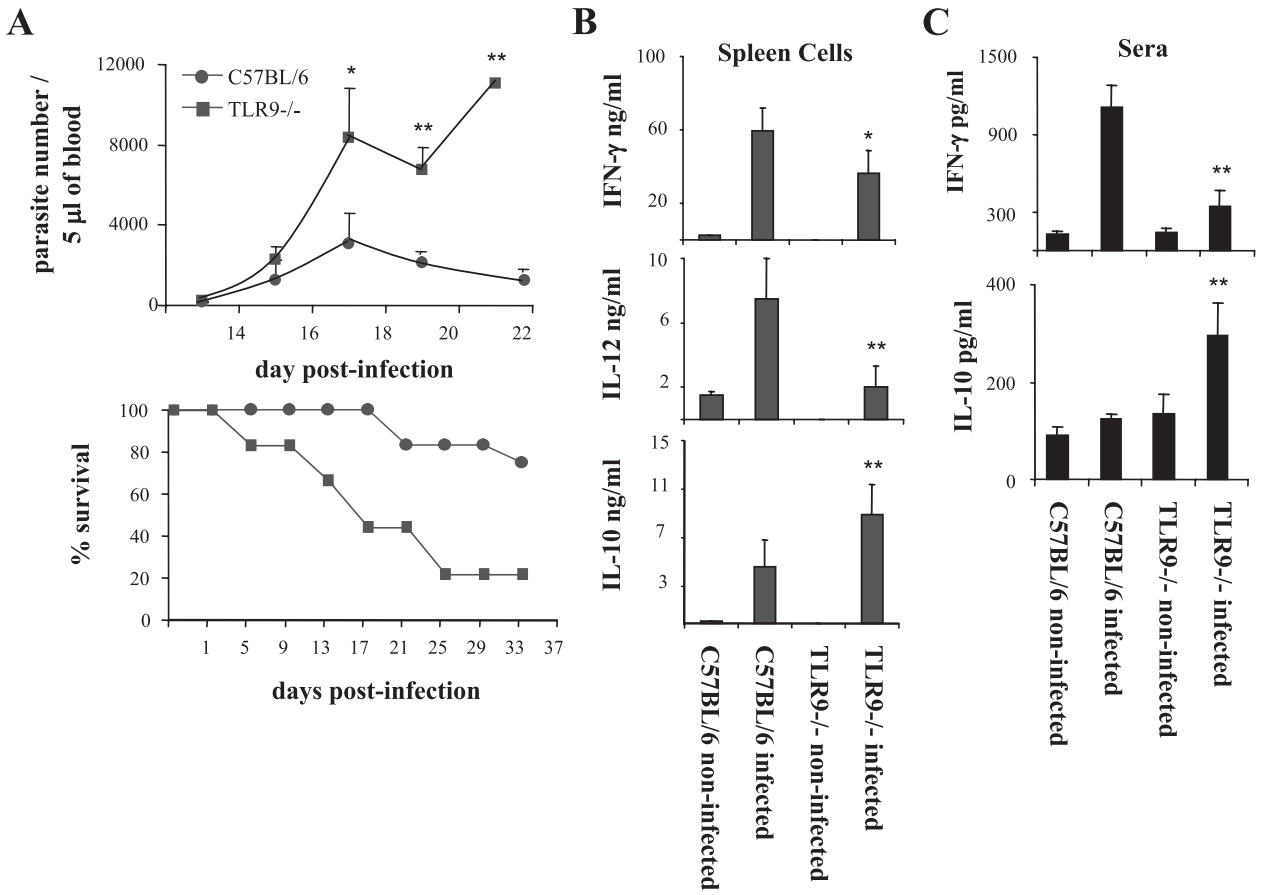


**FIGURE 1.** Enhanced susceptibility and impaired proinflammatory cytokine production in TLR9 deficient mice infected with *T. cruzi*. *A*, WT (C57BL/6) and TLR9$^{-/-}$ mice were infected by i.p. injection with 1,000 blood trypomastigote forms of *T. cruzi* (*top panel*). Parasitemia was evaluated every other day, and cumulative mortality was followed daily (*bottom panel*). Statistical analysis conducted at days 18, 20, and 22 postinfection denotes that the differences in parasitemia (*, $p < 0.05$; **, $p < 0.01$) and survival curves ($p < 0.05$) are significant when comparing TLR9$^{-/-}$ and WT mice. *B* and *C*, A group of five mice were sacrificed 16 days postinfection at the parasitemia peak, and both spleen cells (*B*) and sera (*C*) were harvested for the measurement of cytokine levels. Spleen cells from WT and TLR9$^{-/-}$ were cultured in the absence of additional in vitro antigenic stimulation and supernatant was harvested 48 h later for the measurement of IFN-γ, and IL-12; sera were used for the measurement of IFN-γ and IL-10. The experiment was performed three times, leading to similar results. Asterisks indicate that cytokine production in spleen cell culture or in sera from infected TLR9$^{-/-}$ mice is different when comparing TLR9 and WT mice (*, $p < 0.05$; **, $p < 0.01$).

two CpG motifs. Sequences containing two consecutive mismatches were excluded. Then, a second filter was applied so that no more than three mismatches were allowed in the sequence TCGTCGTT NNNGTCGTT, where N represents any nucleotide. In a second set of criteria, we searched for the motif TCGTCGT(4,5)GTCGTT, where the numbers between parenthesis indicate the number of times the previous nucleotide can be repeated in that position. Again three mismatches were allowed as long as they did involve neither one of the two CpG motifs, and sequences containing two consecutive mismatches were excluded.

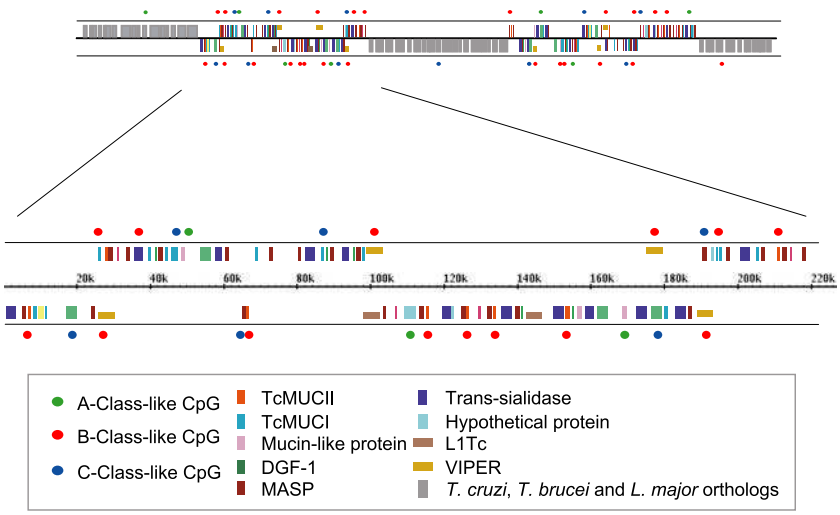


**FIGURE 2.** Prototype of *T. cruzi* genomic regions containing the putative immunostimulatory CpG motifs. The schematic figure shows the concentration of A-like, B-like, and C-like classes of CpG motifs in a *T. cruzi*-specific region containing the retrotransposon VIPER element and genes encoding surface proteins; these motifs are mostly absent from genome areas that encode *T. cruzi*, *T. brucei*, and *L. major* orthologs.

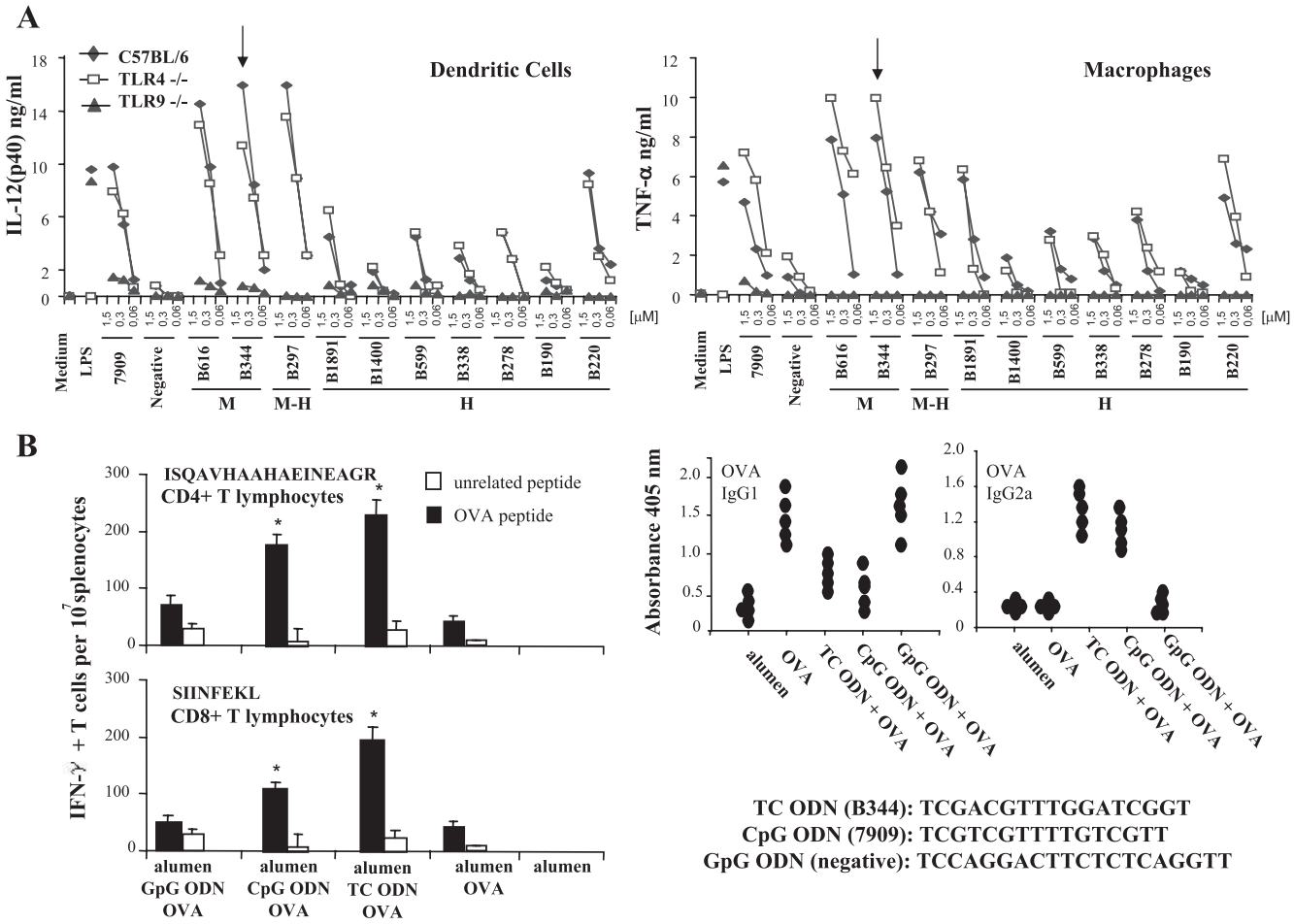


**FIGURE 3.** Potent proinflammatory and in vivo immunological adjuvant activity of B class-like motifs derived from the retrotransposon VIPER elements, *A*, B-class-like ODNs derived from *T. cruzi* genome were synthesized in a phosphorothioate backbone and tested in BMDCs (*left panel*), and inflammatory macrophages (*right panel*) from WT (C57BL/6; filled diamonds), TLR4$^{-/-}$ (open squares), and TLR9$^{-/-}$ (filled triangles). ODNs were tested at different concentrations as indicated and LPS and 7909 ODN were used as positive controls for TLR4 and TLR9 activation, respectively. M, M-H, and H stand for mouse, mouse-human hybrid, and human CpG-like motifs, respectively. IL-12 (p40) and TNF-$\alpha$ were measured in the cell supernatants 24 h after cell stimulation. These experiments were repeated four times, yielding similar results. *B*, BALB/c mice were immunized with alum (alumen) alone, OVA along with alum, alum plus ODN 7909 (positive control), alum plus B344 (a VIPER-derived CpG motif, indicated by an arrow in *A*), or alum plus GpG ODN (negative control), and the ability of CD4$^+$ T and CD8$^+$ T cells to produce IFN-$\gamma$ was analyzed by ELISPOT using the ISQAVHAA HAEINEAGR or SIINFEKL peptides, respectively (*left panels*). In addition, we evaluated in the sera of immunized mice the levels of IgG1 and IgG2a Abs specific for highly purified OVA. Asterisks indicate that the number of IFN-$\gamma$ producing cells is higher in mice immunized with OVA associated with alum and 7909 and B344 ODNs. We used five animals per group. The experiment was repeated two times, yielding similar results.

To identify human TLR9 agonists, we used more stringent criteria. For the identification of *T. cruzi* B-class-like CpG DNA motifs, we searched for the pattern PyPyGTCGTTN(0,4)GTCGTT, where Py stands for pyrimidine, N is any nucleotide, and the numbers between parenthesis indicate the number of times the previous nucleotide can be repeated. Only one mismatch was allowed at the eighth position. To search for C-class-like CpG DNA motifs, we used the previously described nucleotide pattern (27) of TpC at the 5′ end followed by the stimulatory hexameric GTCGTT motif linked to a GC-rich palindromic sequence by a T spacer. One mismatch was allowed as long as the GTCGT sequence was not involved. The A-class-like CpG motifs included the poly(G) tails with phosphorothioate linkages at the 5′ and 3′ ends containing 4–6 guanine residues and a phosphodiester palindromic CpG-containing sequence in the ODN center involving at least six nucleotides (2, 27). We also searched for A-class-lacking poly(G) tails and included the atcgat motif flanked by 3–5 self-complementary bases to generate palindromic sequences involving 12–16 nucleotides that are recognized by TLR9 (28).

### *Luciferase assay*

HEK293 cells stably expressing either human TLR9 or TLR7 and a luciferase gene under the control of the pELAM promoter (containing critical NF-$\kappa$B sites) were used for testing the activity of *T. cruzi*-derived ODNs (25). We also used HEK cells stably transfected with mouse TLR9, human TLR9, human TLR4, or human TLR2, which were transiently transfected with a pGL3 vector containing a firefly luciferase gene under the control of a NF-$\kappa$B promoter and a pRL vector expressing a *Renilla* luciferase gene (Promega) for constitutive protein expression. Cells lysates were mixed with a Dual luciferase reporter assay system (Promega) substrate and relative luciferase units were calculated by normalizing the raw luminescence values to the background (25).

### *Immunization protocols*

OVA (Sigma-Aldrich) and ODNs (Alpha DNA) were adsorbed to alum (Alum; Reheis) at concentrations of 50 and 40 $\mu$g, respectively. Groups of five mice were vaccinated with alum, alum plus OVA, alum plus OVA plus B344, alum plus OVA plus 7909, or alum GpG ODN (negative control) plus OVA, receiving two doses of vaccine at a 15-day interval. Sera and spleens were collected 23 days after the last immunization for analysis of immune responses.

### *IgG measurements*

Vaccinated mice were bled from the retro-orbital plexus under ether anesthesia and sera were stored at −20°C for the measurement of Ab levels by ELISA. Secondary Ab, peroxidase-conjugated goat anti-mouse IgG1 or IgG2a (Sigma-Aldrich), was used and the reactions were detected with 3,3′,5,5′-tetramethylbenzidine reagent (Sigma-Aldrich).

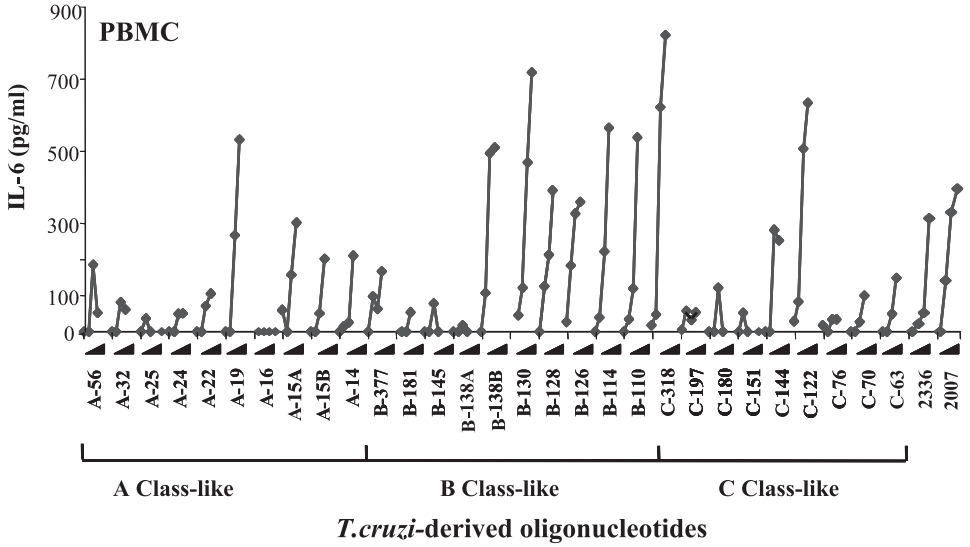


**FIGURE 4.** Proinflammatory activity of human A-, B-, and C-class-like motifs derived *T. cruzi* genome.Human ODNs containing CpG motifs derived from the *T. cruzi* genome were synthesized in a fully phosphorothioate backbone (B- and C-class-like) or, in the case of the A-class-like motif, the central palindromic sequence contained a phosphodiester backbone. The ODNs were tested in association with DOTAP for their activity on PBMCs derived from healthy donors, and the levels of IL-6 were measured in the cell supernatants 24 h after cell stimulation. 2336 and 2007 were used as positive controls for A- and B-class ODNs. Four different concentrations (3.0, 1.0, 0.3, and 0.1 $\mu$M) were used to stimulate PBMCs with each ODN. We performed PBMC experiments in three different donors, yielding similar results.

### *ELISPOT and ELISA for cytokine production assay*

Nitrocellulose bottom, 96-well plates (Millipore) were coated with anti-IFN-$\gamma$ mAb (clone R4-6A2; BD Biosciences) and blocked for 2 h. For T cell stimulation we used the $CD4^+$ T cell epitope (ISQAVAA-HAEINEAGR; 20 $\mu$M) and the $CD8^+$ T cell epitope (SIINFEKL; 200 M). Spleen cells were prepared in complete DMEM supplemented with rIL-2 (100U/ml) and added to plates at $10^6$ cells per well for 20 h. A biotinylated anti-IFN-$\gamma$ mAb (clone XMG1.2; BD Pharmingen) was used to detect cytokine spots in combination with streptavidin-peroxidase conjugate (BD Pharmingen). Spots were revealed with 1 mg/ml 3,3′-diaminobenzidine (Sigma-Aldrich). For cytokine production assays, splenocytes, macrophages, or DCs were prepared as described above, plated at $5 \times 10^6$ cells/ml, and incubated at 37°C and 5% CO2 for 72 h in the presence or absence of various stimuli. IFN-$\gamma$, IL-10, and IL-12 concentrations were determined in cell culture supernatants with DuoSet ELISA (R&D Systems). Two hundred thousand PBMCs were cultured in 96-well plates in the presence of ODNs at different concentrations associated with DOTAP as indicated in the figure legends (Figs. 4, 5, and 7) for 24 h, and IL-6 was measured in the cell culture supernatant with DuoSet ELISA (R&D Systems).

### *Studies of colocalization of live trypomastigotes and TLRs*

Trypomastigotes from CL-Brener expressing RFP were used to infect HEK cells transfected with TLR9 YFP or transduced BMDC expressing human TLR9-YFP. Transfected/transduced cells were infected with 5–50 live tissue culture RFP-trypomastigotes per cell, and colocalization was evaluated with a confocal Leica TCS SP2 microscope (Leica Microsystems) using the sequential scan tool at different time points up to 24 h postinfection.

### *Statistical analysis*

Student′s *t* test or ANOVA was used to analyze the significance of differences in means between groups. Survival curves were generated using the Kaplan-Meier method and the significance of differences was calculated by the log-rank test. Statistical significance was defined as $p < 0.05$. The frequency of the observed vs the expected number of CpG motifs within an specific genomic area considered both the genomic length of a specific segment and the CG content of the *T. cruzi* genome. Statistical significance was calculated using a $\chi^2$ test and defined when $p < 0.0001$.

## Results

### *Mouse- and human-like CpG motifs are concentrated in genes encoding the retrotransposon VIPER sequence and mucin-like glycoproteins, respectively*

The results presented in Fig. 1*A* show that $TLR9^{-/-}$ mice are more susceptible to infection with the CL-Brener (8), the reference strain of the *T. cruzi* genome project, a strain that had its genome completely sequenced (18). Augmented parasitemia and accelerated mortality is associated with impaired synthesis of IL-12 and IFN-$\gamma$ (Fig. 1*B*) by spleen cells as well as IFN-$\gamma$ levels in the sera (Fig. 1*C*) harvested at 16 days postinfection. In contrast, we found an enhanced systemic production of IL-10 in $TLR9^{-/-}$ mice as compared with wild-type (WT) mice infected with *T. cruzi.*

To identify the stimulatory DNA motifs that act as TLR agonists, we took advantage of the sequenced *T. cruzi* genome (CL-Brener strain) (18) and searched for classical B-class-like CpG motifs previously defined in bacteria (2). In an attempt to identify B-class-like CpG motifs that might have stimulatory properties and are slightly distinct from those previously described in bacteria, we used less stringent criteria. Of 254 sequences resembling the mouse GACGTT motif, 170 (~67%) are derived from the retrotransposon VIPER elements associated with regions in the *T. cruzi* genome that are not syntenic with *T. brucei* and *L. major* genes (Table I and Fig. 2). We also found 20 copies of a highly stimulatory motif for mouse TLR9 that was a combination of human and mouse motifs (Table I). Our statistical analysis indicates that the observed frequency of mouse-like immunostimulatory CpG motifs in the VIPER elements was at least 20-fold higher than the expected frequency ($p < 0.0001$; $\chi$ test).

We then performed a more stringent search for well defined human A-, B- and C-class CpG motifs (Table II). A smaller number of A-class-like motifs was identified as compared with B- and C-class-like motifs, and they were not preferentially associated with any specific *T. cruzi* gene. Taking into account the 10 topmost abundant motifs, we found 147 hits for the B-class-like motifs, 115

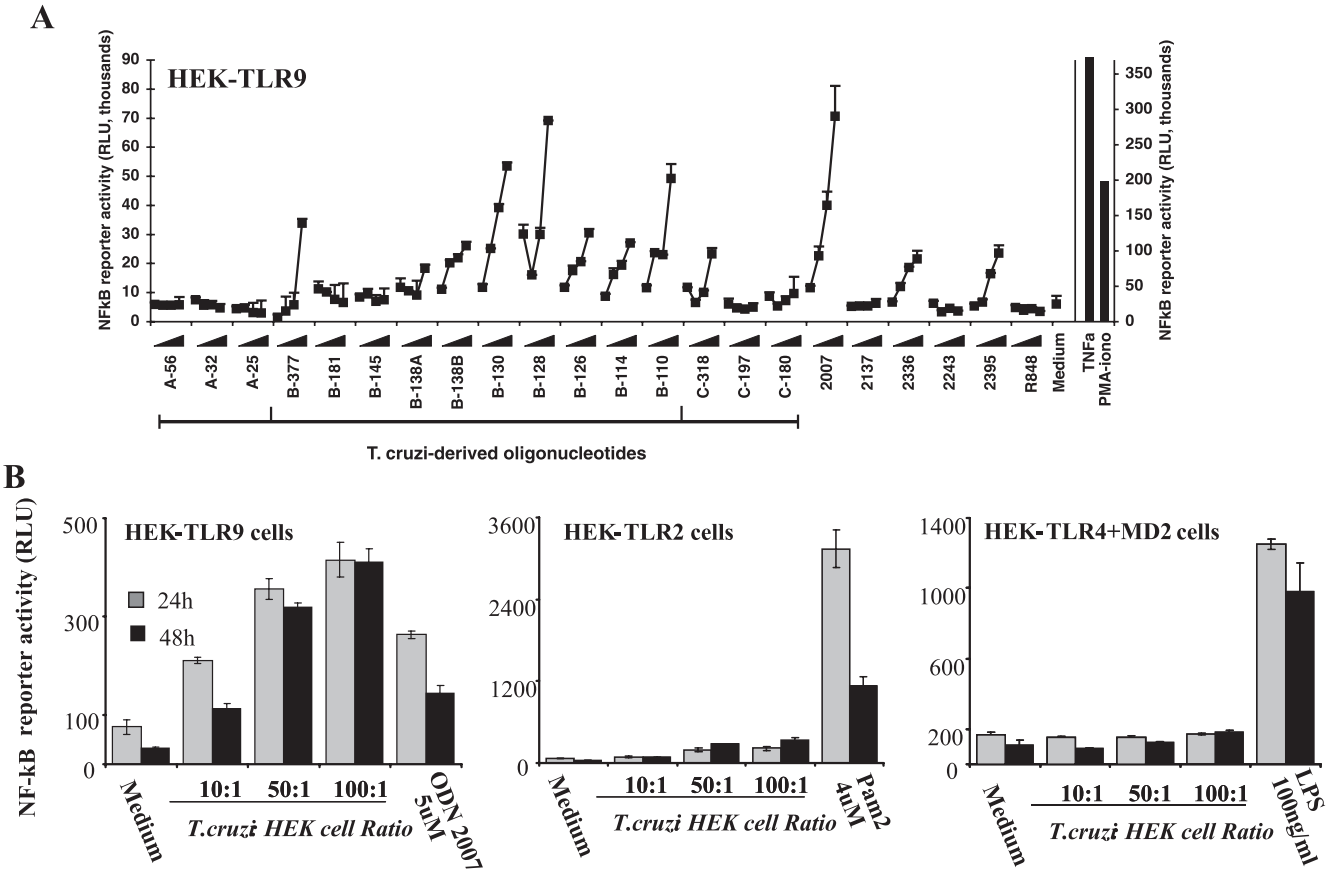


**FIGURE 5.** Invasive *T. cruzi* trypomastigotes colocalize and stimulate host cells via TLR9. *A*, The ODNs containing the human-like motifs were also tested in HEK cells stably transfected with human TLR9 and a luciferase gene under the control of an NF-κB promoter. In the stimulation experiment using transgenic HEK cell lines that overexpress TLR9, we used plain ODNs (i.e., not associated with DOTAP). Parallel stimulation of TLR7-expressing reporter cells, which did not respond to CpG oligos but did respond to the TLR7/8 agonist R848, was used as control, and no response was seen to *T. cruzi*-derived ODNs (data not shown). 2007 (stimulatory B-class CpG), 2137 (nonstimulatory B-class GpC), 2336 (stimulatory A-class CpG), 2243 (nonstimulatory A-class GpC), 2395 (stimulatory C-class), R848 (synthetic TLR7/8 agonist), TNF-α (100 ng/ml), and PMA (10 ng/ml) plus ionomycin (100 ng/ml) were used as controls on HEK cell experiments. We performed two experiments for HEK cells, yielding similar results. *B*, HEK cells stably transfected with either TLR9 (*left panel*), TLR2 (*middle panel*), or TLR4/MD2 (*right panel*) were transiently transfected with plasmids containing firefly luciferase under the control of a NF-κB promoter or *Renilla* luciferase as a constitutively expressed gene. The cells were infected with different numbers of trypomastigotes, and the firefly and *Renilla* luciferase activities were measured 24 (*gray bars*) and 48 h (filled bars) postinfection. The relative luciferase units (RLU) were calculated by normalizing the raw luminescence values to the background. In the stimulation experiment with transgenic HEK cell lines we used ODN 2007 (5 μM), $Pam_3CSK_4$ (4 μM), and LPS (100 ng/ml) as positive controls for agonists of TLR9, TLR2, and TLR4, respectively. Note that we performed three experiments for HEK cells yielding similar results.

for the C-class-like motifs, and only 19 hits for the A-class-like motifs. Importantly, when using the criteria defined by Verthelyi and colleagues (28), which include the atcgat central motif flanked by 3–5 self-complementary bases to generate palindromic sequences involving 12–16 nucleotides and excluding the poly(G) tail at both ends, the frequency of A-class like motifs was raised to 67 hits, but they were still not associated with any particular gene or genome region. As shown in Table II, the majority (~61%) of the coding regions containing the well-defined human B-class-like CpG motifs corresponds to the *mucin* genes (~36 times over the expected frequency; $p < 0.0001$). For human C-class-like motifs, the majority (56%) of the motifs located within coding regions were associated with the *TcMUC* genes (~15 times over expected the frequency; $p < 0.0001$).

### *Immunostimulatory activity of mouse B-class ODN motifs from* T. cruzi *genome*

To analyze the immunostimulatory properties of the selected sequences, the corresponding ODNs containing CpG motifs were synthesized and tested in the immunostimulatory assays. Phosphorothioate ODNs were used because they are more resistant to endonuclease degradation than unmodified ones. As shown in Fig. 3*A*, several ODNs containing CpG motifs derived from the *T. cruzi* genome stimulated a IL-12p40 response by DCs from WT mice. The active CpG ODNs also induced IL-12p70 in the range of 1–2 ng/ml (data not shown). The immunostimulatory activity varied depending on the oligonucleotide sequence. As expected, these effects were abolished in DCs derived from $TLR9^{-/-}$ mice and were sustained in cells from mice lacking TLR4 (Fig. 3*A*), excluding the possible influence of LPS contamination in the ODN preparations. Similar patterns of induction of IL-12p40/p70 (not shown), NO (not shown), and TNF-α (Fig. 3*A*, *right panel*) production were observed using macrophages derived from WT mice, and these effects were abolished in macrophages derived from $TLR9^{-/-}$ animals. These ODNs containing CpG motifs were also tested in human cells; however, a relatively small immunostimulatory effect was detected (Table I).

We next tested the ability of parasite-derived ODNs to promote the development of Th1 responses in vivo, similar to that elicited by infection with *T. cruzi* in mice. We selected the

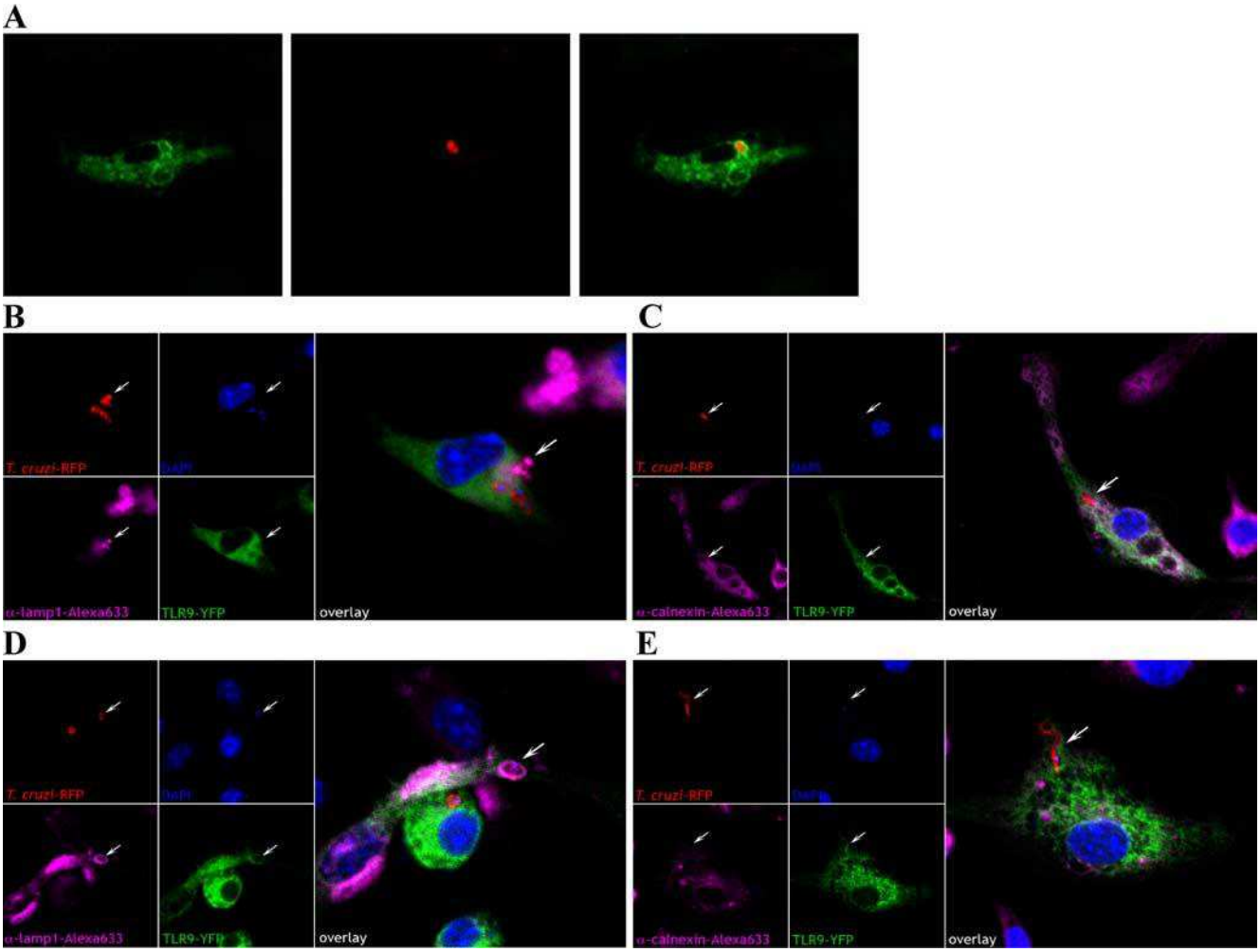


**FIGURE 6.** Subcellular localization of TLR9 in *T. cruzi*-infected BMDCs. *A*, BMDCs transduced with human TLR9-YFP were infected with RFP-*T. cruzi* trypomastigotes at a ratio of 1:50 (host cell:parasite) and analyzed by a confocal Leica TCS SP2 microscope (Leica Microsystems) using the sequential scan tool at different time points up to 24 hs postinfection. *B–E*, BMDCs transduced with YFP-tagged TLR9 were treated with medium alone (*B* and *C*) or medium containing 2 $\mu$M ODN2007 (*D* and *E*) for 30 min and subsequently infected with RFP-expressing *T. cruzi* trypomastigotes. After 1 h, nonbound parasites were washed out and cells were intracellularly stained for the late endosomal/lysosomal marker LAMP-1 (*B* and *D*) or the endoplasmic reticulum-resident protein calnexin (*C* and *E*). In resting cells, internalized parasites were observed in LAMP-1-positive vacuoles (*B*, arrows) that were negative for both TLR9 and calnexin (*C*, arrows). In contrast, CpG-treated cells displayed extensive colocalization of TLR9 with *T. cruzi* parasitophorous vacuoles (*D* and *E*, arrows). These vacuoles were also positive for LAMP-1 and negative for calnexin, indicative of TLR9 translocation from the endoplasmic reticulum to lysosomes.

VIPER sequence that is abundant in the *T. cruzi* genome and highly stimulatory for mouse macrophages and DCs. The results of this experiment are shown in Fig. 3*B*. Mice were immunized with alum alone, OVA and alum, alum plus *T. cruzi*-derived ODN B344 (Table I and Fig. 3*A*), alum plus bacteria-derived ODN (7909), and alum plus ODN with a GpG instead of a CpG motif (negative control). The immune response was analyzed for IFN-$\gamma$ response using ELISPOT and peptides encoding the $CD4^+$ T (ISQAVHAAHAEINEAGR) and $CD8^+$ T epitopes (SIINFEKL). Our results show that the use of a *T. cruzi*-derived ODN dramatically enhanced the ability of both $CD8^+$ T and $CD4^+$ T cells to produce IFN-$\gamma$. Further, the *T. cruzi*-derived ODN also skewed the humoral immune response toward a Th1 phenotype, with a dominant production of OVA-specific Abs of the IgG2a isotype as opposed to a low IFN-$\gamma$ response and a dominant IgG1 response in mice that were immunized with alum alone or in the presence of the negative control ODN. These data are consistent with the importance of immunostimulatory sequences derived from the *T. cruzi* genome, because we observed a lower cytokine (Fig. 1) and Ab (not shown) response in $TLR9^{-/-}$ infected with *T. cruzi.*

### *Immunostimulatory activity of human ODN motifs from the* T. cruzi *genome*

The ten most abundant A-, B- and C-like human CpG motifs found in the *T. cruzi* genome were selected and synthesized and their immunostimulatory properties tested in vitro in HEK cells transfected with either mouse or human TLR9 (Table II and Fig. 5) as well as PBMCs from healthy donors (Fig. 4). For the B- and C-class-like motifs, the ODN sequences were synthesized in a fully phosphorothioate backbone, whereas for the A-class motif the 5′ and 3′ poly(G) ends were phosphorothioate modified and the central palindromic sequence contained the native phosphodiester linkage. The results presented in Fig. 4 show that the stimulation of B-like and, to a lesser extent, C-like motifs derived from the *T. cruzi* genome induced the production of IL-6. We also observed the induction of IFN-$\alpha$ by PBMCs exposed to either A-, B- or

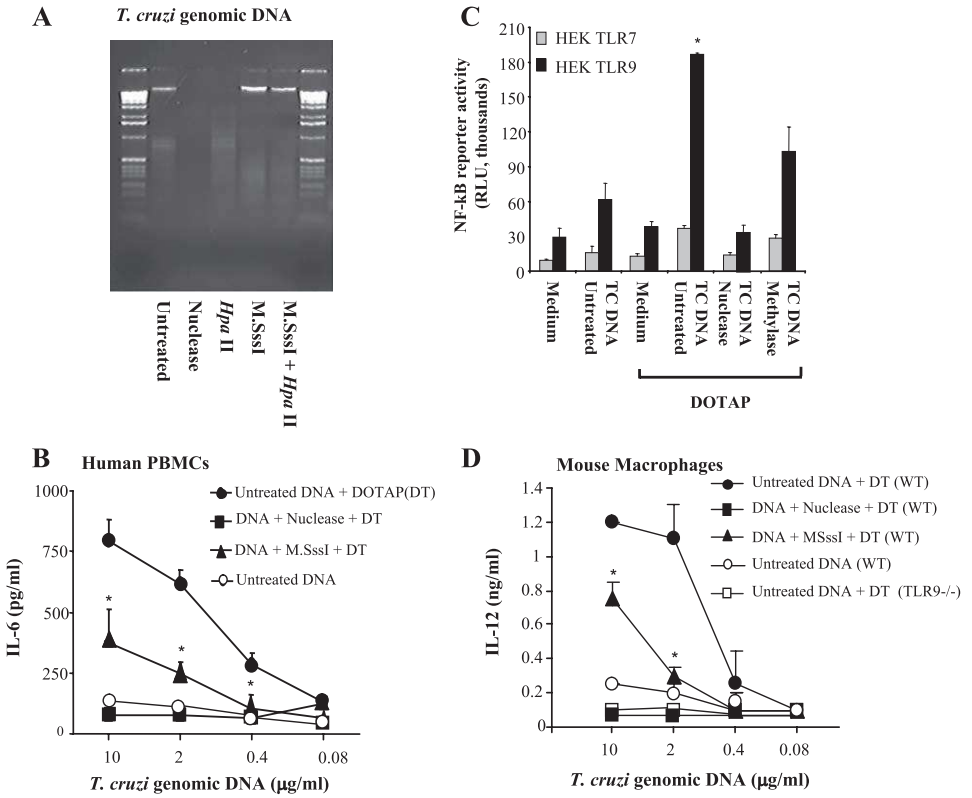


**FIGURE 7.** Potent proinflammatory activity of *T. cruzi* genomic DNA. *A*, *T. cruzi* genomic DNA was extracted from epimastigote forms and left untreated or treated with nuclease, the restriction enzyme *Hpa*II (which cleaves unmethylated CpG motifs), methylase M.SssI, and M.SssI followed by *Hpa*II and analyzed in an agarose-ethidium bromide gel. *B–D*, After treatment, different preparations of parasite DNA were used to stimulate human PBMCs (*B*), HEK cells transfected with TLR9 or TLR7 (*C*), or murine macrophages from WT (C57BL/6) or TLR9$^{-/-}$ associated or not associated with DOTAP (DT) as indicated (*D*). The results are representative of one of two experiments that yielded similar results. Asterisks indicate that cellular activation with *T. cruzi* DNA (TC DNA) associated with DOTAP is significantly higher ($p < 0.05$) than DNA (10 $\mu$g/ml) treated with methylase when given in the same concentration and that *T. cruzi* DNA (10 $\mu$g/ml) associated with DOTAP is higher ($p < 0.05$) than DNA (10 $\mu$g/ml) without DOTAP or than DNA (10 $\mu$g/ml) treated with either nuclease or methylase when given to the cells associated with DOTAP (*C*).

C-like *T. cruzi*-derived ODNs, in particular when ODNs were associated with DOTAP (data not shown).

### *Infection with* T. cruzi *stimulates NF-κB mediated responses in HEK cells transfected with TLR9*

To demonstrate that the *T. cruzi* ODNs containing human motifs were indeed stimulating TLR9, we used the HEK cells stably co-transfected with a NF-κB-controlled luciferase reporter plasmid and human TLR9 or TLR7 as control. Fig. 5*A* shows that most of the human B-class-like ODNs were highly active in HEK cells transfected with TLR9, but not in those transfected with TLR7 (data not shown). As previously shown for A- and C-class ODNs, the *T. cruzi*-derived A- and C-class-like ODNs were inactive in stimulating NF-κB-mediated responses in HEK cells transfected with TLR9. Nevertheless, they were active when delivered to host cells with DOTAP (not shown). Importantly, Fig. 5*B*, *left panel*, shows that *T. cruzi* parasites stimulate, in a dose-dependent activity, HEK cells transfected with TLR9. In contrast, we observed a small to nil ability of live *T. cruzi* parasites to elicit a NF-κB-dependent response in HEK cells transfected with TLR2 (Fig. 5*B*, *middle panel*). Further, HEK cells transfected with MD2/TLR4 (Fig. 5*B*, *right panel*), which express high levels of DAI-1 (not shown), did not respond to *T. cruzi* infection.

### *TLR9 and* T. cruzi *colocalization in host cells*

Importantly, mouse BMDCs transduced with a chimeric human TLR9-YFP were infected with RFP-expressing *T. cruzi* trypomastigotes (22), and TLR9-parasite colocalization was evaluated. Fig. 6*A* demonstrates that, 4 h postinfection of transduced DCs, we evidenced colocalization of RFP-parasites and TLR9-YFP. It is known that TLR9 is constitutively expressed in the endoplasmatic reticulum and recruited to the endo-lysosomal compartment after cellular activation with a TLR9 agonist (6). Therefore, we exposed transduced DCs to a TLR9 agonist and evaluated TLR9 colocalization with RFP-transgenic parasites. At an early stage of infection (1 h postinfection) we observed no colocalization of parasite, TLR9, and LAMP-1 (Fig. 6, *B* and *C*). However, when cells were preactivated with TLR9 agonist, we observed intense colocalization of TLR9, LAMP-1, and RFP-expressing parasites as early as 1 h postinfection (Fig. 6, *D* and *C*). In any instance, no colocalization of parasites and TLR9 was observed in the endoplasmic reticulum (Fig. 6). Thus, we favor the hypothesis that *T. cruzi* promotes TLR9 recruitment to lysosomes, where this cognate receptor encounters DNA released from the parasite during the process of invasion/uptake by phagocytic cells.

### *Endo-lysosomal delivery potentiates proinflammatory activity of* T. cruzi *genomic DNA in both mouse and human cells that express TLR9*

Genomic *T. cruzi* DNA has been shown to stimulate the synthesis of proinflammatory cytokines by murine macrophages and DCs (8, 15). However, the amount of DNA required for this proinflammatory activity is very high, i.e., in the range of 50 $\mu$g/ml. The gel presented in Fig. 7*A* shows that parasite genomic DNA before and

after treatment with nuclease, methylase, and *Hpa*II. *T. cruzi* DNA was completely degraded by nuclease digestion and became resistant to *Hpa*II after treatment with methylase (Fig. 7*A*, M.SssI). *Hpa*II cut unmethylated CpG motifs. We demonstrated that *T. cruzi* DNA activity on human PBMCs is very low when up to 10 $\mu$g/ml DNA is used (Fig. 7*B*). Nevertheless, when we transfected *T. cruzi* genomic DNA into human PBMCs with DOTAP, a liposomal transfection reagent, we observed a dramatic increase in the immunostimulatory properties of the parasite DNA as measured by the induction of IL-6 (Fig. 7*B*) and IFN-$\alpha$ (data not shown). Importantly, the activity was diminished by the treatment of DNA with methylase and completely abolished by the treatment with nuclease (Fig. 7*B*). *T. cruzi* genomic DNA associated with DOTAP also triggered the expression and activity of the luciferase gene under the control of NF-$\kappa$B elements in HEK cells transfected with human TLR9. Finally, our results also show that when combined, DOTAP and *T. cruzi* DNA stimulate IL-12p70 production by macrophages from WT but not from TLR9$^{-/-}$ mice (Fig. 7*D*).

## Discussion

TLR9 was initially identified as a main mammalian innate immune receptor involved in the recognition of unmethylated CpG motifs derived from bacterial genomic DNA, which have been widely used as vaccine adjuvants and immunotherapeutic compounds in experimental protocols (1–3). Furthermore, in conjunction with other TLRs that recognize nucleic acids (i.e., TLR3, TLR7, and TLR8), TLR9 constitutes a main stream of innate immune receptors involved in the recognition of viruses (3, 29–31). Recent studies indicate that TLR9 also has an important role during infection with protozoan parasites, including *T. cruzi*, the etiologic agent of Chagas disease (7–10). In this study we address two main questions regarding the recognition of *T. cruzi* DNA by TLR9: 1) what are the main immunostimulatory DNA sequences and how they are distributed in the parasite genome; and 2) what is the cellular compartment where *T. cruzi* encounters TLR9. Our results show that TLR9 (7–10) is most likely triggered by unmethylated CpG regions found in the *T. cruzi* genome. Intriguingly, the most active and abundant immunostimulatory CpG motifs identified in this study were derived from the retrotransposon VIPER elements found in the *T. cruzi* genome. We also demonstrated that infection with *T. cruzi* parasites promotes recruitment of TLR9 to the endo-lysosome compartment, where they probably interact during the initial steps of parasite invasion/uptake by phagocytes. Consistently, the immunostimulatory activity was highly enhanced when *T. cruzi* DNA was delivered to the endo-lysosomal compartment of host cells expressing TLR9.

In a survey of 15 bacterial species, the immunostimulatory capacity of bacterial DNA samples directly correlated with the frequency of CpG dinucleotides (32). In that study, the CpG frequency ranged from 1.44 to 12.21%. The frequency of CpG dinucleotide sequences in the *T. cruzi* genome is 4.6%, which puts it within the range seen for bacterial DNA. Mammalian DNA is thought to be less immunostimulatory compared with bacterial DNA because the frequency of the CpG motif is suppressed. In addition, mammalian, but not bacterial, DNA is highly methylated (3). Although mammals and protozoa share membership in the eukaryotic kingdom, we found that CpG motifs in *T. cruzi* DNA had a low level of methylation. Importantly, methylation of *T. cruzi* genomic DNA with the methylase named M.SssI partially abolishes cellular activation by TLR9. Thus, these findings suggest the involvement of unmethylated CpG motifs in the proinflammatory activity of protozoa DNA.

Importantly, by analyzing the available *T. cruzi* genomic sequences (18) we found a high number of CpG motifs (Fig. 2) that were similar but not identical with the ones previously defined in bacterial DNA (2). In addition, the CpG motifs were not evenly distributed in the *T. cruzi* genome, being preferentially associated to regions of the genome that contains *T. cruzi*-specific genes, including those encoding surface proteins, and not so frequent in areas that encode *T. cruzi*, *T. brucei*, and *L. major* ortholog genes. Consistent with the hypothesis that TLRs specific for nucleic acids may have evolved to detect viruses, we found that the highly immunostimulatory ODNs were associated with the multiple copies of the retro-element VIPER, inserted in the trypanosomatid founder lineage after the divergence of *Leishmania* and *Trypanosoma* (33). These retroelements and RNA viruses share a common ancestor (34).

Three main classes of the immunostimulatory CpG DNA motifs that activate human TLR9 have been described. B-class CpG ODNs are the most potent inducers of proinflammatory cytokines. In addition, the CpG B-class motifs are also strong stimulators of B cell responses (2). In contrast, CpG A-class ODN has been defined as a weaker inducer of proinflammatory cytokines but a strong inducer of type I IFN (IFN-$\alpha$ and IFN-$\beta$) (35). C-class CpG ODNs combine the immunostimulatory properties of both the A-class and the B-class, having the ability of stimulating B cell response, proinflammatory cytokines, and IFN type I production. Consistent with the ability of the parasite to elicit a strong proinflammatory response (e.g., high levels of IL-12, IFN-$\gamma$, and TNF-$\alpha$) (11, 12, 36) and an intense activation of B cells and hypergammaglobulinemia (11, 37, 38), we found that the *T. cruzi* genome contains elevated copy numbers of B-class-like sequences, both for human and mouse motifs. Besides the crucial role of IFN-$\gamma$ (type II) in controlling of the parasite infection, it has been shown that production of IFN-$\alpha/\beta$ (type I) is increased in *T. cruzi*-infected human fibroblasts (39). Furthermore, it was recently shown that type I IFN stimulates NO synthesis during early stages of *T. cruzi* infection, contributing to the control of the parasitemia (40, 41). Importantly, our experiments (data not shown) also demonstrate that parasite-derived DNA as well as A-, B-, and C-class-like CpG ODNs, when delivered using a cationic lipid (DOTAP), leads to endo-lysosomal activation of the type I IFN pathway as previously reported by using otherwise inactive B-class CpG motifs (42).

An alternative innate immune receptor for pathogen DNA is the recently discovered DAI-1, a cytosolic receptor that recognizes dsDNA and induces type I IFN as well as NF-$\kappa$B-mediated responses (43). Although we cannot exclude the role of DAI-1 in the response of PBMCs to *T. cruzi*-derived DNA or CpG ODNs, we have no evidences that DAI-1 is involved in the innate immune responses studied here. First, in our PBMC experiments we used the DOTAP a transfection reagent that preferentially delivers DNA/ODNs to the endo-lysosomal compartment. Second, we only observed the response of HEK cells, which express high levels of DAI-1, to *T. cruzi* infection or parasite-derived DNA/CpG ODNs when they were transfected with TLR9. Third, DCs and macrophages, from TLR9$^{-/-}$ mice, which also express DAI-1, were nonresponsive to parasite-derived DNA or CpG ODNs.

During active cell invasion, trypomastigotes enter the vertebrate host cell by either recruitment and fusion of lysosomes at the plasma membrane (44) or through invagination of the plasma membrane followed by intracellular fusion with lysosomes (45). Regardless of the entry route, lysosomal fusion is essential to retain the parasite inside the host cell and therefore establish a productive infection (46). Alternatively, parasites are taken up by professional phagocytic cells and driven to the phagolysosomes. Importantly, TLR9 normally resides in the endoplasmic reticulum membranes, but when exposed to stimulatory CpG motifs it is

quickly recruited to the endo-lysosome compartment (6). Thus, we also addressed the question regarding the host cell compartment in which the *T. cruzi* encounters TLR9. By using RFP-expressing parasites and HEK cells/DCs transfected/transduced with chimera TLR9-YFP, we evaluated the colocalization and activation of TLR9 by *T. cruzi*. Although TLR9 is primarily expressed by professional phagocytic cells, we also observed NF-κB activation in TLR9-transfected HEK cells infected with *T. cruzi.* Further, activation of host cells expressing TLR9 is mainly observed when we use live trypomastigotes. Thus, we presume that active host cell invasion by trypomastigotes is a key event for TLR9 activation during infection with *T. cruzi.* In our confocal microscopy analysis we clearly observed a colocalization of TLR9 and invasive parasites ~4–6 h postinfection. Further, we observed that preactivation with a TLR9 agonist resulted in a significant increase in the number of events/fields where parasites and TLR9 were colocalized. By using anti-LAMP-1 (late-endosomal/lysosomal marker) and anti-calnexin (endoplasmic reticulum marker), we demonstrate that parasites and TLR9 colocalize in the endo-lysosomes. These findings are consistent with the fact that the parasite DNA has to be delivered into the endo-lysosomal compartment to activate TLR9 as indicated by experiments demonstrating the ability of the DOTAP transfection reagent to enhance the activation of TLR9 by parasite-derived genomic DNA or CpG ODNs. We assume that parasites, which are eventually destroyed during this initial process of invasion/uptake by professional phagocytic cells (41), release DNA that will become available to TLR9 into lysosome-fused vacuoles.

Taking into account the hypothesis that B-class-like CpG motifs may indeed play an important role during protozoan infections, we performed a comparative analysis of the genome from different protozoan parasites. It was clear that both *T. cruzi* and *T. gondii* have the higher contents, both for human and mouse B-class-like CpG motifs, followed by *L. major* and *T. brucei* and finally by *P. falciparum*, which corresponded to the CG/AT content of parasite genome (47, 48). In this regard, it is intriguing that the most abundant and immunostimulatory CpG motifs were found associated with the retrotransposon VIPER element, which is largely distributed in the *T. cruzi* genome. The role of this retrotransposon has been attributed to the control of gene expression and possibly genome flexibility (49, 50). Based on our results, we speculate that the maintenance of multiple copies of the retrotransposon VIPER may offer additional advantage in *T. cruzi* adaptation to the host and evolution by eliciting cell-mediated immunity and control of parasite replication, avoiding vertebrate host lethality, and leading to long-term parasitism and perpetuation of the parasite life cycle.

## Acknowledgments

We are grateful to Dr. Andrea M. Macedo for contribution in generating the RFP transgenic *T. cruzi* strain, Joseph Conlon for help with HEK293 mouse TLR9 experiments, and João Luis Reis Cunha for help with *T. cruzi* genome analysis. We also acknowledge Drs. Alan Sher, Andre Bafica, Stuart Levitz, and Daniela Verthelyi for critically reading the manuscript and offering suggestions and Dr. Najib El-Sayed and the *T. cruzi* sequencing consortium for make available the CL-Brener individual reads and annotated contigs used in this study.

## Disclosures

The authors have no financial conflict of interest.

## References

1. Hemmi, H., O. Takeuchi, T. Kawai, T. Kaisho, S. Sato, H. Sanjo, M. Matsumoto, K. Hoshino, H. Wagner, K. Takeda, and S. Akira. 2000. A Toll-like receptor recognizes bacterial DNA. *Nature* 408: 740–745.
2. Krieg, A. M. 2002. CpG motifs in bacterial DNA and their immune effects. *Annu. Rev. Immunol.* 20: 709–760.
3. Akira, S., S. Uematsu, and O. Takeuchi. 2006. Pathogen recognition and innate immunity. *Cell* 124: 783–801.
4. Abe, T., H. Hemmi, H. Miyamoto, K. Moriishi, S. Tamura, H. Takaku, S. Akira, and Y. Matsuura. 2005. Involvement of the Toll-like receptor 9 signaling pathway in the induction of innate immunity by baculovirus. *J. Virol.* 79: 2847–2858.
5. Wikstrom, F. H., B. M. Meehan, M. Berg, S. Timmusk, J. Elving, L. Fuxler, M. Magnusson, G. M. Allan, F. McNeilly, and C. Fossum. 2007. Structure-dependent modulation of α interferon production by porcine circovirus 2 oligodeoxyribonucleotide and CpG DNAs in porcine peripheral blood mononuclear cells. *J. Virol.* 81: 4919–4927.
6. Latz, E., A. Schoenemeyer, A. Visintin, K. A. Fitzgerald, B. G. Monks, C. F. Knetter, E. Lien, N. J. Nilsen, T. Espevik, and D. T. Golenbock. 2004. TLR9 signals after translocating from the ER to CpG DNA in the lysosome. *Nat. Immunol.* 5: 190–198.
7. Drennan, M. B., B. Stijlemans, J. Van den Abbeele, V. J. Quesniaux, M. Barkhuizen, F. Brombacher, P. De Baetselier, B. Ryffel, and S. Magez. 2005. The induction of a type 1 immune response following a *Trypanosoma brucei* infection is MyD88 dependent. *J. Immunol.* 175: 2501–2509.
8. Bafica, A., H. C. Santiago, R. Goldszmid, C. Ropert, R. T. Gazzinelli, and A. Sher. 2006. Cutting edge: TLR9 and TLR2 signaling together account for MyD88-dependent control of parasitemia in *Trypanosoma cruzi* infection. *J. Immunol.* 177: 3515–3519.
9. Parroche, P., F. N. Lauw, N. Goutagny, E. Latz, B. G. Monks, A. Visintin, K. A. Halmen, M. Lamphier, M. Olivier, D. C. Bartholomeu, et al. 2007. Malaria hemozoin is immunologically inert but radically enhances innate responses by presenting malaria DNA to Toll-like receptor 9. *Proc. Natl. Acad. Sci. USA* 104: 1919–1924.
10. Gazzinelli, R. T., and E. Y. Denkers. 2006. Protozoan encounters with Toll-like receptor signalling pathways: implications for host parasitism. *Nat. Rev. Immunol.* 6: 895–906.
11. Golgher, D., and R. T. Gazzinelli. 2004. Innate and acquired immunity in the pathogenesis of Chagas disease. *Autoimmunity* 37: 399–409.
12. Campos, M. A., M. Closel, E. P. Valente, J. E. Cardoso, S. Akira, J. I. Alvarez-Leite, C. Ropert, and R. T. Gazzinelli. 2004. Impaired production of proinflammatory cytokines and host resistance to acute infection with *Trypanosoma cruzi* in mice lacking functional myeloid differentiation factor 88. *J. Immunol.* 172: 1711–1718.
13. Campos, M. A., I. C. Almeida, O. Takeuchi, S. Akira, E. P. Valente, D. O. Procopio, L. R. Travassos, J. A. Smith, D. T. Golenbock, and R. T. Gazzinelli. 2001. Activation of Toll-like receptor-2 by glycosylphosphatidylinositol anchors from a protozoan parasite. *J. Immunol.* 167: 416–423.
14. Oliveira, A. C., J. R. Peixoto, L. B. de Arruda, M. A. Campos, R. T. Gazzinelli, D. T. Golenbock, S. Akira, J. O. Previato, L. Mendonca-Previato, A. Nobrega, and M. Bellio. 2004. Expression of functional TLR4 confers proinflammatory responsiveness to *Trypanosoma cruzi* glycoinositolphospholipids and higher resistance to infection with *T. cruzi*. *J. Immunol.* 173: 5688–5696.
15. Shoda, L. K., K. A. Kegerreis, C. E. Suarez, I. Roditi, R. S. Corral, G. M. Bertot, J. Norimine, and W. C. Brown. 2001. DNA from protozoan parasites *Babesia bovis*, *Trypanosoma cruzi*, and *T. brucei* is mitogenic for B lymphocytes and stimulates macrophage expression of interleukin-12, tumor necrosis factor α, and nitric oxide. *Infect. Immun.* 69: 2162–2171.
16. Harris, T. H., N. M. Cooney, J. M. Mansfield, and D. M. Paulnock. 2006. Signal transduction, gene transcription, and cytokine production triggered in macrophages by exposure to trypanosome DNA. *Infect. Immun.* 74: 4530–4537.
17. Hirschfeld, M., Y. Ma, J. H. Weis, S. N. Vogel, and J. J. Weis. 2000. Cutting edge: repurification of lipopolysaccharide eliminates signaling through both human and murine toll-like receptor 2. *J. Immunol.* 165: 618–622.
18. El-Sayed, N. M., P. J. Myler, D. C. Bartholomeu, D. Nilsson, G. Aggarwal, A. N. Tran, E. Ghedin, E. A. Worthey, A. L. Delcher, G. Blandin, et al. 2005. The genome sequence of *Trypanosoma cruzi*, etiologic agent of Chagas disease. *Science* 309: 409–415.
19. Camargo, E. P. 1964. Growth and differentiation in *Trypanosoma cruzi*: I. Origin of metacyclic trypanosomes in liquid media. *Rev. Inst. Med. Trop. Sao Paulo* 12: 93–100.
20. Teixeira, S. M., K. Otsu, K. L. Hill, L. V. Kirchhoff, and J. E. Donelson. 1999. Expression of a marker for intracellular *Trypanosoma cruzi* amastigotes in extracellular spheromastigotes. *Mol. Biochem. Parasitol.* 98: 265–270.
21. DaRocha, W. D., R. A. Silva, D. C. Bartholomeu, S. F. Pires, J. M. Freitas, A. M. Macedo, M. P. Vazquez, M. J. Levin, and S. M. Teixeira. 2004. Expression of exogenous genes in *Trypanosoma cruzi*: improving vectors and electroporation protocols. *Parasitol. Res.* 92: 113–120.
22. Pires, S. F., W. D. DaRocha, J. M. Freitas, L. A. Oliveira, G. T. Kitten, C. R. Machado, S. D. Pena, A. E. Chiari, A. M. Macedo, and S. M. Teixeira. 2008. Cell culture and animal infection with distinct *Trypanosoma cruzi* strains expressing red and green fluorescent proteins. *Int. J. Parasitol.* 38: 289–297.
23. Camargo, M. M., I. C. Almeida, M. E. Pereira, M. A. Ferguson, L. R. Travassos, and R. T. Gazzinelli. 1997. Glycosylphosphatidylinositol-anchored mucin-like glycoproteins isolated from *Trypanosoma cruzi* trypomastigotes initiate the synthesis of proinflammatory cytokines by macrophages. *J. Immunol.* 158: 5890–5901.
24. Qin, Z., G. Noffz, M. Mohaupt, and T. Blankenstein. 1997. Interleukin-10 prevents dendritic cell accumulation and vaccination with granulocyte-macrophage colony-stimulating factor gene-modified tumor cells. *J. Immunol.* 159: 770–776.
25. Latz, E., A. Verma, A. Visintin, M. Gong, C. M. Sirois, D. C. Klein, B. G. Monks, C. J. McKnight, M. S. Lamphier, W. P. Duprex, et al. 2007. Ligand-induced conformational changes allosterically activate Toll-like receptor 9. *Nat. Immunol.* 8: 772–779.

26. Hartmann, G., R. D. Weeratna, Z. K. Ballas, P. Payette, S. Blackwell, I. Suparto, W. L. Rasmussen, M. Waldschmidt, D. Sajuthi, R. H. Purcell, et al. 2000. Delineation of a CpG phosphorothioate oligodeoxynucleotide for activating primate immune responses in vitro and in vivo. *J. Immunol.* 164: 1617–1624.
27. Vollmer, J. 2006. CpG motifs to modulate innate and adaptive immune responses. *Int. Rev. Immunol.* 25: 125–134.
28. Puig, M., A. Grajkowski, M. Boczkowska, C. Ausin, S. L. Beaucage, and D. Verthelyi. 2006. Use of thermolytic protective groups to prevent G-tetrad formation in CpG ODN type D: structural studies and immunomodulatory activity in primates. *Nucleic Acids Res.* 34: 6488–6495.
29. Alexopoulou, L., A. C. Holt, R. Medzhitov, and R. A. Flavell. 2001. Recognition of double-stranded RNA and activation of NF-κB by Toll-like receptor 3. *Nature* 413: 732–738.
30. Diebold, S. S., T. Kaisho, H. Hemmi, S. Akira, and E. S. C. Reis. 2004. Innate antiviral responses by means of TLR7-mediated recognition of single-stranded RNA. *Science* 303: 1529–1531.
31. Heil, F., H. Hemmi, H. Hochrein, F. Ampenberger, C. Kirschning, S. Akira, G. Lipford, H. Wagner, and S. Bauer. 2004. Species-specific recognition of single-stranded RNA via toll-like receptor 7 and 8. *Science* 303: 1526–1529.
32. Dalpke, A., J. Frank, M. Peter, and K. Heeg. 2006. Activation of Toll-like receptor 9 by DNA from different bacterial species. *Infect. Immun.* 74: 940–946.
33. Lorenzi, H. A., G. Robledo, and M. J. Levin. 2006. The VIPER elements of trypanosomes constitute a novel group of tyrosine recombinase-encoding retrotransposons. *Mol. Biochem. Parasitol.* 145: 184–194.
34. Xiong, Y., and T. H. Eickbush. 1990. Origin and evolution of retroelements based upon their reverse transcriptase sequences. *EMBO J.* 9: 3353–3362.
35. Krug, A., S. Rothenfusser, V. Hornung, B. Jahrsdorfer, S. Blackwell, Z. K. Ballas, S. Endres, A. M. Krieg, and G. Hartmann. 2001. Identification of CpG oligonucleotide sequences with high induction of IFN-α/β in plasmacytoid dendritic cells. *Eur. J. Immunol.* 31: 2154–2163.
36. Michailowsky, V., N. M. Silva, C. D. Rocha, L. Q. Vieira, J. Lannes-Vieira, and R. T. Gazzinelli. 2001. Pivotal role of interleukin-12 and interferon-γ axis in controlling tissue parasitism and inflammation in the heart and central nervous system during *Trypanosoma cruzi* infection. *Am. J. Pathol.* 159: 1723–1733.
37. d'Imperio Lima, M. R., H. Eisen, P. Minoprio, M. Joskowicz, and A. Coutinho. 1986. Persistence of polyclonal B cell activation with undetectable parasitemia in late stages of experimental Chagas' disease. *J. Immunol.* 137: 353–356.
38. Reina-San-Martin, B., W. Degrave, C. Rougeot, A. Cosson, N. Chamond, A. Cordeiro-Da-Silva, M. Arala-Chaves, A. Coutinho, and P. Minoprio. 2000. A B-cell mitogen from a pathogenic trypanosome is a eukaryotic proline racemase. *Nat. Med.* 6: 890–897.
39. de Avalos, S. V., I. J. Blader, M. Fisher, J. C. Boothroyd, and B. A. Burleigh. 2002. Immediate/early response to *Trypanosoma cruzi* infection involves minimal modulation of host cell transcription. *J. Biol. Chem.* 277: 639–644.
40. Costa, V. M., K. C. Torres, R. Z. Mendonca, I. Gresser, K. J. Gollob, and I. A. Abrahamsohn. 2006. Type I IFNs stimulate nitric oxide production and resistance to Trypanosoma cruzi infection. *J. Immunol.* 177: 3193–3200.
41. Koga, R., S. Hamano, H. Kuwata, K. Atarashi, M. Ogawa, H. Hisaeda, M. Yamamoto, S. Akira, K. Himeno, M. Matsumoto, and K. Takeda. 2006. TLR-dependent induction of IFN-β mediates host defense against *Trypanosoma cruzi*. *J. Immunol.* 177: 7059–7066.
42. Honda, K., Y. Ohba, H. Yanai, H. Negishi, T. Mizutani, A. Takaoka, C. Taya, and T. Taniguchi. 2005. Spatiotemporal regulation of MyD88-IRF-7 signalling for robust type-I interferon induction. *Nature* 434: 1035–1040.
43. Takaoka, A., Z. Wang, M. K. Choi, H. Yanai, H. Negishi, T. Ban, Y. Lu, M. Miyagishi, T. Kodama, K. Honda, et al. 2007. DAI (DLM-1/ZBP1) is a cytosolic DNA sensor and an activator of innate immune response. *Nature* 448: 501–505.
44. Tardieux, I., P. Webster, J. Ravesloot, W. Boron, J. A. Lunn, J. E. Heuser, and N. W. Andrews. 1992. Lysosome recruitment and fusion are early events required for trypanosome invasion of mammalian cells. *Cell* 71: 1117–1130.
45. Woolsey, A. M., L. Sunwoo, C. A. Petersen, S. M. Brachmann, L. C. Cantley, and B. A. Burleigh. 2003. Novel PI 3-kinase-dependent mechanisms of trypanosome invasion and vacuole maturation. *J. Cell Sci.* 116: 3611–3622.
46. Andrade, L. O., and N. W. Andrews. 2004. Lysosomal fusion is essential for the retention of *Trypanosoma cruzi* inside host cells. *J. Exp. Med.* 200: 1135–1143.
47. Gardner, M. J., N. Hall, E. Fung, O. White, M. Berriman, R. W. Hyman, J. M. Carlton, A. Pain, K. E. Nelson, S. Bowman, et al. 2002. Genome sequence of the human malaria parasite *Plasmodium falciparum*. *Nature* 419: 498–511.
48. El-Sayed, N. M., P. J. Myler, G. Blandin, M. Berriman, J. Crabtree, G. Aggarwal, E. Caler, H. Renauld, E. A. Worthey, C. Hertz-Fowler, et al. 2005. Comparative genomics of trypanosomatid parasitic protozoa. *Science* 309: 404–409.
49. Vazquez, M., C. Ben-Dov, H. Lorenzi, T. Moore, A. Schijman, and M. J. Levin. 2000. The short interspersed repetitive element of *Trypanosoma cruzi*, SIRE, is part of VIPER, an unusual retroelement related to long terminal repeat retrotransposons. *Proc. Natl. Acad. Sci. USA* 97: 2128–2133.
50. Bhattacharya, S., A. Bakre, and A. Bhattacharya. 2002. Mobile genetic elements in protozoan parasites. *J. Genet.* 81: 73–86.